Robust Segmentation and Volumetric Registration in a Multi-view 3D Freehand Ultrasound Reconstruction System

Honggang Yu, Marios S. Pattichis
image and video Processing and Communications Lab
Department of Electrical and Computer Engineering
The University of New Mexico
Albuquerque, NM 87131, USA

M.Beth Goens
Pediatric Cardiology Clinic of the Children's Hospital
Heart Center
The University of New Mexico
Albuquerque, NM 87131, USA

Abstract—In this paper, we present a new reconstruction method with volumetric registration and semi-automatic segmentation in a multi-view 3D freehand ultrasound imaging system. The new volumetric registration approach is performed on binarized walls using non-linear least squares. It can provide accurate multi-view reconstructions despite significant rigid target motion between different acoustic window acquisitions.

A hybrid adaptive gradient vector flow (GVF) geometric active contour (GAC) model is used for image sequence segmentation. It allows for relatively simple initialization of the deformable model, while avoiding edge leaking at poor edges and small boundary gaps.

The algorithms were validated on four ultrasound phantom data sets (eight sequences of a total of 336 images) and two echocardiography data sets (four sequences for a total of 75 images). Quantitative evaluation shows that automatic segmentation is comparable with manual segmentation. Using breath-holding and cardiac gating, volume estimates from multi-view reconstructions of the left-ventricle were found to be in better agreement with clinical estimates than volumes estimated from single view reconstructions.

Keywords – multiple acoustic windows, echocardigraphy, registration, segmentation, three-dimensional reconstruction.

I. INTRODUCTION

Freehand 3D ultrasound imaging techniques can be used to reconstruct 3D anatomy from a set of registered 2D image slices. The 2D slices can be located at any arbitrary orientation and position throughout 3D space, and can be acquired using any standard, 2D ultrasound transducer in conjunction with a spatial locator. Most prior research in echocardiography has been focused on using a single acoustic window view for reconstructing the left ventricle. However, for a single view, there are fundamental limitations that degrade the reconstruction, such as the presence of shadows due to bones (ribs) and air (in the lungs) that lead to reconstructions that do not have sufficient information to reflect the original anatomy.

Recently, there has been increased interest in the use of multiple acoustic windows for providing 3D reconstructions of the left ventricle. Ye *et al.* [1] used a 3D rotational probe and an electromagnetic spatial locator to combine data from an apical long-axis view and a parasternal short-axis view. Their method assumed that there was a good spatial alignment between different view sweeps. Leotta *et. al.* [2] used a 2D freehand scanning protocol to combine parasternal and apical windows *in vitro*. The 2D images were manually registered by manual tracing of the left ventricular boundaries. A similar study and system was reported by Legget *et al.* [3].

None of these studies addressed the problem of how to automatically register 3D reconstructions between different acoustic windows. In the research presented in this paper, we present a new multi-view reconstruction methodology with volumetric registration between different acoustic windows and semi-automatic sequence segmentation using gradient vector flow (GVF) geometric active contour (GAC) model. We have reported on earlier versions of our system in our previous publications [4-6]. In this paper, we provide extensive mathematical details on the new volumetric registration method. In [6], for single images, we provided comparisons between the new segmentation method and the other related geometric deformable models. In this paper, we extend the work to 2D+T image sequence segmentation and present results from extensive validation.

Section 2 describes the registration and segmentation methods in detail. Section 3 presents the validation results on phantom and pediatric echocardiography data. Concluding remarks and future work are given in Section 4.

II. METHODS

A. *Imaging System*

All imaging was performed using a 7MHz 1D wide-view array transducer probe 7V3C and A 2D ultrasound machine, the Acuson Sequoia C256 (Siemens, USA). The spatial locations of 2D image slices were recorded by a six-degree of freedom DC electromagnetic position and orientation measurement device, the Flock of Birds (FOB) (Ascension, Burlington, VT, USA).

1-4244-0785-0/06/$20.00

B. 3D Reconstruction with volumetric registration

Automatic registration is a required and important step for combining acquisitions between different acoustic windows. We note that rigid movement of the target in inter-view sweeps and inaccurate sensor measurements cause the majority of the registration errors [7]. Intra-view deformation generated by respiration and cardiac motion can be solved by breath-holding and ECG gating.

We developed a new automatic volumetric registration method in our multi-view reconstruction system. First, we initialize the search for the optimal registration parameters using a 3D Hotelling transform (also called Principal Component Analysis or Karhunen-Loeve transform) to construct an object-based reference volume, to coarsely register 3D volumes from different views. Then, we perform a higher accuracy registration using a robust, non-linear least squares method (Levenberg-Marquardt) to estimate the optimal registration parameters. We have found that the new registration strategy is very efficient and robust. It converges to the same registration parameters from a wide variety of initializations [5].

We note that echocardiography images of the same anatomy but acquired from different acoustic windows can appear substantially different. The majority of the pixels in 2D echocardiography images exhibit non-constant features, especially inside the endocardial cavity, where we have muscle tissue, blood flow, severe speckle noise and many other artifacts (such as shadowing). Thus, registration with the original intensity images is not likely to succeed. Instead, we used the manually or semi-automatically segmented object to binarize the ECG-gated endocardial boundaries. The underlying assumption is that the endocardial boundaries should be common features among different acoustic window images.

In the following we will define terminology that will be used to describe the algorithm. Suppose we want to register two sets of 2D image sequences acquired at two different views, view V_1 and view V_2. Let N_p, N_q be the number of pixels inside the wall boundaries in sets P, Q, respectively. Let P points come from view V_1 and Q points come from view V_2 as given by

$$P = \{\mathbf{p}_i\}, \qquad i = 1, 2, \cdots, N_p$$
$$Q = \{\mathbf{q}_j\}, \qquad j = 1, 2, \cdots, N_q$$

where $\mathbf{p}_i$, $\mathbf{q}_j$ are 3D vectors, the 3D voxel coordinates from the two sweep views:

$$\mathbf{p}_i = [x_i, y_i, z_i]^T,$$
$$\mathbf{q}_j = [x_j, y_j, z_j]^T.$$

To estimate the parameters of the registration, we considered rigid-body motions, described by translation and rotation as given by:

$$\mathbf{r} = [x, y, z, \alpha, \beta, \gamma]^T$$

where x, y, z are translation distances and α, β, γ are orientation angles.

For the registration method to converge, the complex surface structures from different views must exhibit some partial overlap. Once the feature of data sets are determined, we first reconstruct the 3D view with the largest number of 2D slice planes (denoted by V_1) over a regular Cartesian grid, and then register the 2D slice planes from the rest of the views to it.

The data points from a second view (denoted by V_2) were translated and rotated using a registration transformation. Let $T(\mathbf{q}_j)$ denote the registration transformation. We interpolate the intensity values at $T(\mathbf{q}_j)$ using the image points of $I(\mathbf{p}_i)$ in a 3D Cartesian grid volume. We use the symbol $I(\mathbf{p}_{T(\mathbf{q}_j)})$ to represent the transformed view. The optimal registration vector is estimated as the one that minimizes the mean square error objective function:

$$f(\mathbf{r}) = \frac{1}{N_y} \sum_{j=1}^{N_y} \left\| I(\mathbf{q}_j) - I(\mathbf{p}_{T(\mathbf{q}_j)}) \right\|^2 .$$

In our multi-view reconstruction system, we first averaged all registered single view 3D acquisitions and we then interpolated using tessellation based linear interpolation.

C. Semi-automatic segmentation

In pediatric cardiology, there can be significantly topological variability on the wall boundaries. Furthermore, due to the wide variability in possible abnormal cases, it is difficult to provide significant populations for each abnormal classification. This difficulty in segmentation can be addressed using GVF geometric active contours (GAC).

We developed a new hybrid semi-automatic segmentation strategy on echocardiography sequences, which combines a recently introduced GVF Fast GAC model [8] and a modified level sets methods applied to echocardiography data by Corsi *et al.* [9]. We call it the adaptive GVF GAC model. The advantage of this approach is that it allows for relatively simple initialization of the deformable model, while avoiding edge leaking at poor edges and small boundary gaps.

Corsi *et al.* [9] applied level set techniques to semi-automatically segment 3D echocardiographic data using:

$$\varphi_t = g\varepsilon\kappa|\nabla\varphi| + \beta\nabla g \bullet \nabla\varphi .$$

Here, g is usually defined as an enhanced edge indicator applied to a Gaussian smoothed echocardiography image, given by

$$g = \frac{1}{1+\left(\frac{\left|\nabla\left(G_\sigma\left(x,y\right)*I\left(x,y\right)\right)\right|}{\alpha}\right)^2}.$$

We noticed that Corsi *et al.* dropped the expansion term in the speed function, which controls curve motion in the normal direction. This term could have pushed the evolving curve past boundary gaps. However, we have observed that this approach worked well only when the initial curve was sufficiently close to the actual boundary. To overcome this weakness, we considered integrating GVF in a GAC model.

Here, we note that the GVF force has a large capture range and allows deformable models to be initialized far away from the object boundary [10]. Paragios used a fast GVF GAC model that is robust with respect to the initial conditions, and also allows active contours to undergo topological changes to track multiple objects [8]. In his case, we have:

$$\varphi_t = g\left[\varepsilon\kappa\left|\nabla\varphi\right| - \left(\left(u(x,y), v(x,y)\right)\bullet\nabla\varphi\right)\right]$$

where the vector field $\left(u(x,y), v(x,y)\right)$ is the GVF vector field. It diffuses the image gradient information toward the homogenous background. It is a bidirectional flow that propagates the curve toward the object boundary from inside or outside the boundary. This deformable model allows for convergence over a wide range of initial curves. In the above formulation, the edge indicator function g (instead of β) is used for controlling the strength of the advection term. In the implementation of the method, the strength of the GVF term is decreased when the evolving front approaches the object boundary. But the maximal coefficient of the GVF term is the maximal value of g, which has a value of one in homogeneous regions.

Note that this approach still suffers from boundary leakage artifacts. In our new approach, we recommend a hybrid method that can achieve accurate segmentation without edge leakage, starting from a simple curve initialization. The hybrid new approach relies on the use of Paragios' method for propagating the initial curve closer to the image boundary. When the segmentation curve approaches the real boundary, propagation proceeds with Corsi's method that provides for an accurate result.

The new deformable model is then given by:

$$\varphi_t = g\varepsilon\kappa\left|\nabla\varphi\right| - (1-s)\left[\beta_1\left(\left(u,v\right)\bullet\nabla\varphi\right)\right] + s\beta_2\nabla g\bullet\nabla\varphi$$

where $s = s\left(f\left(x,y\right),t\right)$ is a step function that is a function of the edge map and time. When the step function s is zero, the equation reduces to Paragios' method. When the step function s approaches one, the equation reduces to Corsi's method. Initially, under the new GVF GAC deformable model, the advection term is a GVF field. It drives the evolving curve move fast toward the object boundary even in a homogeneous field. When the segmentation curve is sufficiently close to the true boundary, the edge map assumes higher values. To detect that the evolving curve is approaching the target boundary, at each iteration, we evaluate the average value of the edge map over the current zero level-set. When the average value is above a certain threshold, we turn on the step function. The advection term is then dominated by the vector field ∇g, which can be used to avoid edge leaking on the poor endocardial boundaries and small boundary gaps. The procedure is summarized as:

$$s\left(f\left(x,y\right),t\right) = \begin{cases} 0, & \text{if for all } t' < t: \underset{\varphi(x,y,t')=0}{E}\left(f\left(x,y\right)\right) < T_{thres} \\ 1, & \text{otherwise} \end{cases}$$

where $f\left(x,y\right)$ is the image map function defined as:

$$f(x,y) = \left(\frac{\left|\nabla(G_\sigma(x,y)*I(x,y))\right|}{\alpha}\right)^2.$$

To determine the threshold T_{thres}, we estimate an approximate average value of the edge map over the segmentation boundary. This is estimated from the average value of the edge map over a training set of manually segmented images.

III. Results

A. Data Sets

We used both in-vitro phantom data sets (3D Ultrasound Calibration Phantom, Model 055, CIRS, USA) and in-vivo pediatric heart data sets. Eight sequences of long-axis and short-axis view phantom image video (total 336 images) and four echocardiography sequences of parasternal short-axis and apical long-axis views were used (two were standard 2D B-scan video sequences and the other two also had spatial locator data information).

B. 3D reconstruction with automatic registration

Breath-holding and ECG gating were used to minimize the deformation from cardiac motion in echocardiography data acquisitions. Each single acoustic window sweep lasted about 15 seconds (433 images), which is a much shorter scanning time than the acquisition time reported by Ye *et al.* [1]. The human subjects did not have to remain still in the time it took to switch to a different acoustic window. In our system, the new reconstruction method can automatically correct arbitrary rigid movement between different acoustic window sweeps.

We have shown that by using the new automatic registration method, the two view reconstruction from the parasternal short-axis and apical long-axis view gave a much better representation of the left ventricle compared to each single view reconstructions. The quantitative measurements of left ventricle volume using new reconstruction method are also in better agreement with the standard 2D clinical measurements than single view reconstruction estimates [5].

C. Semi-automatic segmentation

In the segmentation experiments, we set parameters empirically as $\alpha = 0.1, \varepsilon = 0.8, \beta_1 = \beta_2 = 6$. First, we evaluated the performance of the new sequence segmentation method on eight sets of phantom image sequences.

We required that the users provided a rough, initial curve on one arbitrary frame in the image sequence, to initialize the segmentation. Normally, we initialize the segmentation procedure on an image in the middle of the sequence. The segmentation procedure then proceeds to automatically segment images before and after the middle image. Each frame segmentation is initialized by using the segmentation result from the previous frame, allowing for a quick convergence.

Fig. 1 shows a phantom image sequence with fairly low image contrast and high level of speckle noise and the segmentation results using the new GVF GAC method.

To quantitatively validate the segmentation results, we used three evaluation methods. First, the correlation coefficient was calculated between the areas enclosed by the new model generated boundaries and the areas enclosed by manually outlined boundaries. Second, we computed the Hausdorff distance and third, the mean absolute distance (MAD) to measure the difference between the manual and automatic segementation boundaries [11]. The Hausdorff distance measures the distance between the points on two curves that differ the most, while MAD provides the mean difference between the two curves.

All quantitative evaluations are shown in Table Ⅱ. In the last column of table, we present the percentage of successfully segmented images (via visual inspection) as a fraction of all the images that were acquired (normally 40 to 50 image frames) in the sequence.

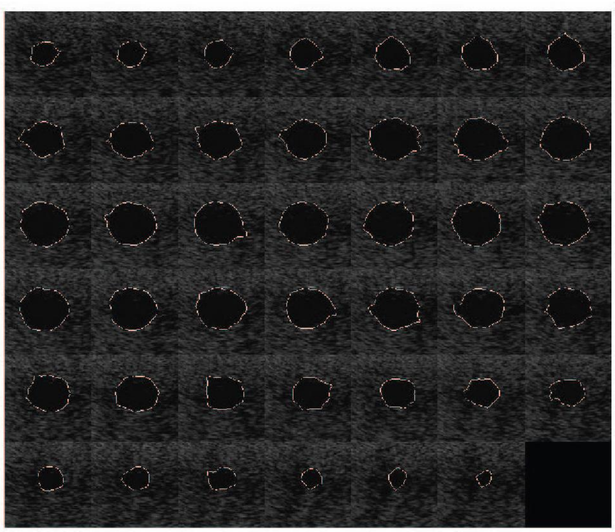

Figure 1. Phantom image sequence segmentation.

TABLE I. PHANTOM SEQUENCESE SEGMENTATION VALIDATION

Sequences	MAD(mm)	Haudorff Distance (mm)	Correlation Coefficient of Area	Percent
1 (40 frames)	0.983 (σ =0.496)	3.108 (σ =2.017)	0.9593	87.5%
2 (40 frames)	0.654 (σ =0.388)	1.423 (σ =0.815)	0.9880	77.5%
3 (40 frames)	0.786 (σ =0.516)	2.719 (σ =2.043)	0.9860	90.0%
4 (40 frames)	0.480 (σ =0.293)	1.198 (σ =0.753)	0.9947	72.5%
5 (44 frames)	0.510 (σ =0.230)	2.175 (σ =1.117)	0.9961	81.8%
6 (41 frames)	0.469 (σ =0.229)	1.963 (σ =0.991)	0.9926	78.1%
7 (44 frames)	0.477 (σ =0.168)	1.847 (σ =1.116)	0.9946	86.4%
8 (47 frames)	0.388 (σ =0.165)	1.591 (σ =0.844)	0.9949	87.2%

For the two echocardiography image sequences, we picked the sequences to cover a full cardiac motion cycle (ES-ED-ES). Both of the sequences from the parasternal and apical views have 26 frames. The parasternal short-axis view sequence segmentations are shown in Fig. 2. During the sequence segmentation, we used visual inspection of each image to judge whether it had been successfully segmented or not. If one of the frames in the sequence did not show acceptable segmentation, we had to reinitialize that frame to restart a segmentation procedure for it and the following frames. The results in Fig. 2 show that the new semi-automatic segmentation method performed well.

Table Ⅲ shows the mean and standard deviation of the MAD and Hausdorff distance of the two echocardiography sequences segmentation. We note that eventhough the two sequences segmentations have similar correlation coefficients for the enclosed area; the distance error measurements (MAD and Hausdorff distance) have a relatively bigger difference.

TABLE II. ECHOCARDIOGRAPHY SEQUENCE SEGMENTATION VALIDATION

Echocardiograpy Sequences	MAD (mm)	Haudorff Distance (mm)	Correlation Coefficient of Area
Parasternal (26 frames)	0.794 (σ =0.272)	3.656 (σ =1.210)	0.9814
Apical (26 frames)	1.267 (σ =0.266)	4.261 (σ =0.899)	0.9802

IV. CONCLUSION

Multi-view freehand acquisitions can provide more complete coverage of the target object anatomy. Unlike previous methods, our new approach does not require that there is good spatial alignment between the different view sweeps, and it does not require manual registration by the users. Accurate reconstruction is achieved through a new geometric registration method, which is performed in a fully automatic mode.

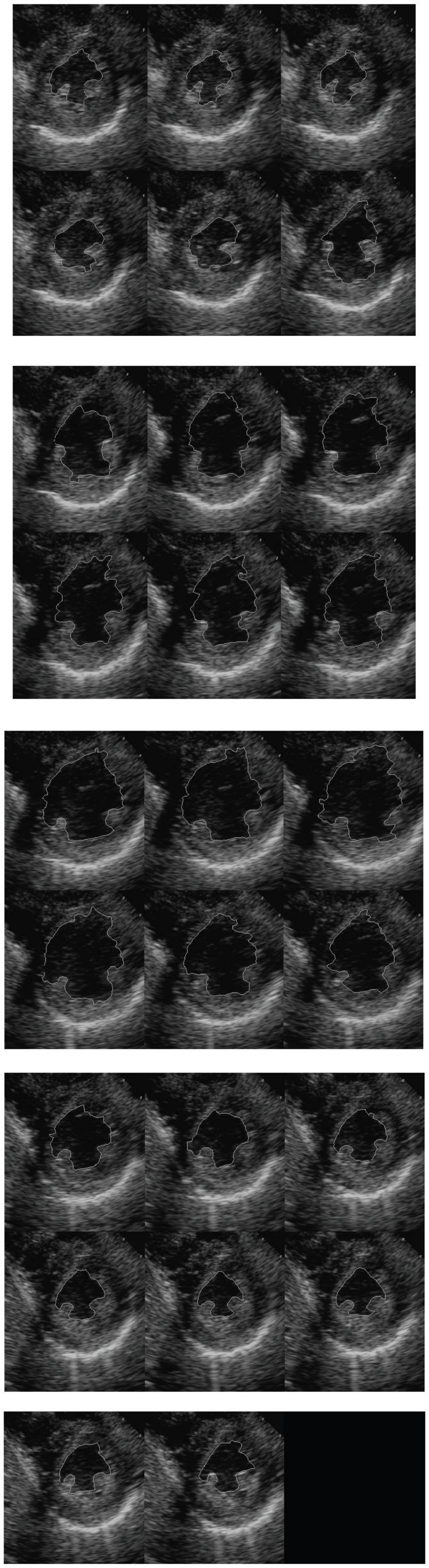

Figure 2. Parasternal short-axis sequence segmentation.

The new adaptive GVF GAC segmentation algorithm has proven to be robust in segmenting objects with significant level of speckle noise, weak edges, and small gaps that are often associated with echocardiography images. As the results show, the new method is insensitive to the initialization of the deformable curve and avoids edge leaking. It allows for quick convergence and accurate segmentation.

An extension of this work is to validate on more echocardiography data sets acquired from multiple acoustic windows. A more objective and accurate comparison would be to compare left ventricle volumes and other cardiac parameters with cardiac magnetic resonance (MR) data.

References

[1] X. Ye, J. A. Noble, and D. Atkinson, "3-D freehand echocardiography for automatic left ventricle reconstruction and analysis based on multiple acoustic windows," *IEEE Transactions on Medical Imaging*, vol. 21, pp. 1051-1058, 2002.

[2] D. F. Leotta, B. Munt, E. L. Bolson, C. Kraft, R. W. Martin, C. M. Otto, and F. H. Sheehan, "Three-Dimensional Echocardiography by Rapid Imaging from Multiple Transthoracic Windows: In Vitro Validation and Initial In Vivo Studies," *Journal of the American Society of Echocardiography*, vol. 10, pp. 830-840, 1997.

[3] M. E. Legget, D. F. Leotta, E. L. Bolson, J. A. McDonald, R. W. Martin, X. N. Li, C. M. Otto, and F. H. Sheehan, "System for quantitative three-dimensional echocardiography of the left ventricle based on a magnetic-field position and orientation sensing system," *IEEE transactions on Biomedical Engineering*, vol. 45, pp. 494-504, 1998.

[4] H. Yu, M. S. Pattichis and M. B. Goens, "A Robust Multi-view Freehand Three-dimensional Ultrasound Imaging System Using Volumetric Registration", *in Proc. of the IEEE International Conference on System, Man and Cybernetics,* vol. 4, pp 3106 – 3111, 2005

[5] H. Yu, M. S. Pattichis and M. B. Goens, "Multi-view 3D Reconstruction with Volumetric Registration in a Freehand Ultrasound Imaging System", in Proc. of the SPIE International Symposium on Medical Imaging. Vol, 6147-6, 2006

[6] H. Yu, M. S. Pattichis and M. B. Goens, "Robust Segmentation of Freehand Ultrasound Image Slices Using Gradient Vector Flow Fast Geometric Active Contours", *in Proc. of the 2006 IEEE Southwest Symposium on Image Analysis and Interpretation*, pp 115-119, 2006

[7] R. Rohling, A. Gee, and L. Berman, "3-D spatial compunding of ultrasound images," *Medical Image Analysis*, vol. 1, pp. 177-193, 1997.

[8] N. Paragios, O. Mellina-Gottardo, and V. Ramesh, "Gradient vector flow fast geometric active contours," *IEEE Transactions on Pattern Analysis and Machine Intelligence*, vol. 26, pp. 402-407, 2004.

[9] C. Corsi, G. Saracino, A. Sarti, and C. Lamberti, "Left ventricular volume estimation for real-time three-dimensional echocardiography," *IEEE Transactions on Medical Imaging*, vol. 21, pp. 1202-1208, 2002.

[10] C. Xu and J. L.Prince, "Snakes, shapes, and gradient vector flow," *IEEE Transactions on Image Processing*, vol. 7, pp. 359-369, 1998.

[11] V. Chalana and Y. Kim, "A Methodology for Evaluation of Boundary Detection Algorithms on Medical Images," *IEEE Transactions on Medical Imaging*, vol. 16, pp. 642-652, 1997.